CHARACTERISTICS OF A SIMPLE, HIGH-RESOLUTION FLOW CYTOMETER BASED ON A NEW FLOW CONFIGURATION

TORE LINDMO AND HARALD B. STEEN, *Department of Biophysics, Norsk Hydro's Institute for Cancer Research, Montebello, Oslo 3, Norway*

ABSTRACT A new flow configuration allows a flow cytometer of high resolution and stability to be assembled from an inverted fluorescence microscope with incident illumination, a pulse photometer, and a multichannel pulse height analyzer. A nozzle produces a hydrodynamically focused sample stream in a liquid jet that is directed onto a microscope cover glass in front of the microscope objective. The microscope provides a mechanically stable optical system of high numerical aperture (N.A.) (oil immersion, N.A. = 1.3) for focusing the excitation light and collection of the fluorescence light.

The instrument has wide optima with regard to the various characteristics of the flow configuration, such as the rate of sample analysis and sheath flow, and the angle of incidence of the liquid jet, thus making it easy to adjust for optimal performance. DNA histograms of rat thymocytes stained with ethidium bromide and mithramycin demonstrate that all angles of incidence can be used. Large-angle incidence (70°) gives the best resolution, i.e., a coefficient of variance (CV) of 0.9% of the peak of the histogram. This is only slightly better than values obtained at other angles, e.g., CV = 1.3% at vertical (0°) incidence. It is concluded that instrumental resolution is equal to or better than CV = 0.9%. Linearity (proportionality between channel number and fluorescence intensity) is within 1%, and instrumental drift over a 1-h period is normally <1–2%.

INTRODUCTION

Flow cytometry has become widely used for quantitative measurements of cellular constituents (1). Usually, the method is based on fluorometry, i.e., the cells are stained with a fluorochrome that binds specifically to the component of interest, e.g., DNA. The cellular content of this constituent is quantitated by measuring the intensity of fluorescence light emitted when the cell passes through the sensor region of a fluorometer. Monodisperse cells carried through the sensor region in a fast liquid flow can be analyzed at a rate exceeding 10^3 cells/s.

The resolution of flow cytometers has steadily been improved. In measurement of cellular DNA content, histograms having a coefficient of variance (CV) (standard deviation relative to mean value) as low as 0.8–1.0% have been recorded (2–6). Parallel to the improvement in resolution, the analytical capacity of flow cytometers has been further developed, and multiparameter instruments with sorting capabilities are now commercially available. However, multiparameter flow cytometers with high power laser light sources and sorting capabilities are complex instruments that are difficult to adjust and operate because the accessibility to the sensor and sorting region has to be restricted for safety reasons. Hence, there is a need

for less complex instrumentation, e.g., to relieve flow sorters of some of the purely analytical tasks or to serve as introductory instruments.

This paper describes a new flow configuration implemented on an inverted fluorescence microscope with incident illumination to form a flow cytometer that compares favorably with most flow cytometers in ease of operation, resolution, and stability. The microscope with its incident light illuminator provides an optical system that is mechanically stable, easy to use, and that gives high sensitivity due to the large numerical aperture (N.A.=1.3) of its oil immersion objective. In contrast to the flow chambers of other microscope-based flow cytometers (6–8), the present flow configuration utilizes a nozzle that produces a liquid jet in air. The sample stream, hydrodynamically focused (9) within the liquid jet, is directed onto a microscope cover glass in front of the microscope objective. The jet may be directed vertically onto the cover glass (i.e., jet parallel to the optical axis), or at certain angle of incidence (up to 70°). A brief description of the instrument and its performance at 70° angle of incidence is given elsewhere (10). Some components of the flow cytometer described in this report were installed to determine more precisely the optimal performance characteristics of the instrument, and are not necessary for normal use.

INSTRUMENT DESCRIPTION

Sensor Region

A laminar sample stream through the sensor region of the instrument is created by directing the jet of liquid from a 80-μm Diam nozzle (Specialty Glass Products Inc., Willow Grove, Pa., part no. 91216) onto a cover glass at a certain angle of incidence, as illustrated in Fig. 1. The sample stream emerges from a 26-gauge platinum needle inlet and is confined to the central part of the liquid jet by the principle of hydrodynamic focusing of sample and sheath flow (9). A hypodermic needle (gauge 21) connected by a tube to an evacuated waste container drains the liquid from the cover glass. The cover glass rests on a

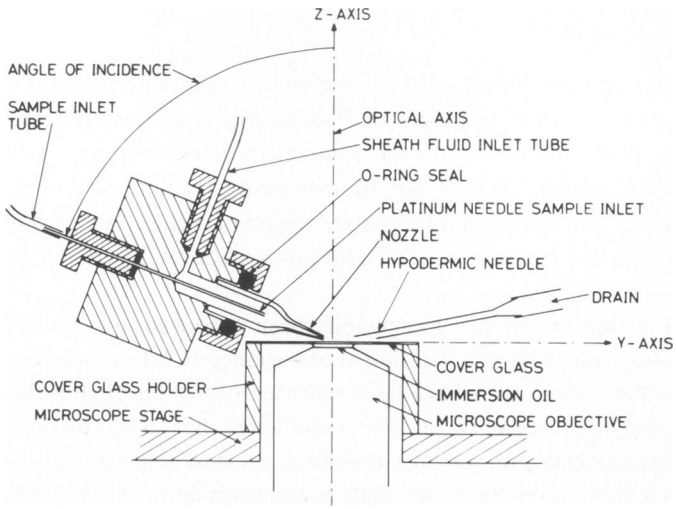

FIGURE 1 Nozzle assembly and sensor region. The nozzle may be rotated around the X-axis (normal to paper plane), thus varying the angle of incidence between 70° (as shown) and 0° (vertical incidence).

holder such that the upper side of the glass is at the normal working distance of the oil immersion objective of an inverted microscope with incident illumination.

The nozzle is mounted on the stage of the microscope, with micrometers for fine adjustments of the position in the X- and Y-directions. The mount allows the nozzle to be rotated around the X-axis (normal to the paper plane, see Fig. 1) with the nozzle tip remaining about 1 mm from the origin of the coordinate system of Fig. 1. Thus, the angle of incidence may be varied between 70°, as shown in Fig. 1, and 0°, i.e., vertical incidence.

Fig. 2 shows the view of the flow on the cover glass as seen in the microscope at the largest angle of incidence (i.e., 70°, panel A) and vertical incidence (i.e., 0°, panel B). At oblique incidence, the sample flow on the cover glass (Y-direction) is confined to a sector <10 μm wide. At vertical incidence, a circular disk of 1–2 mm Diam with laminar liquid flow is created around the point where the liquid jet hits the cover glass, and the sample stream fans out in all directions in the X-Y-plane. Fluorescence is detected with the microscope focused slightly above the cover glass, i.e., when the picture appears as in Fig. 2 B.

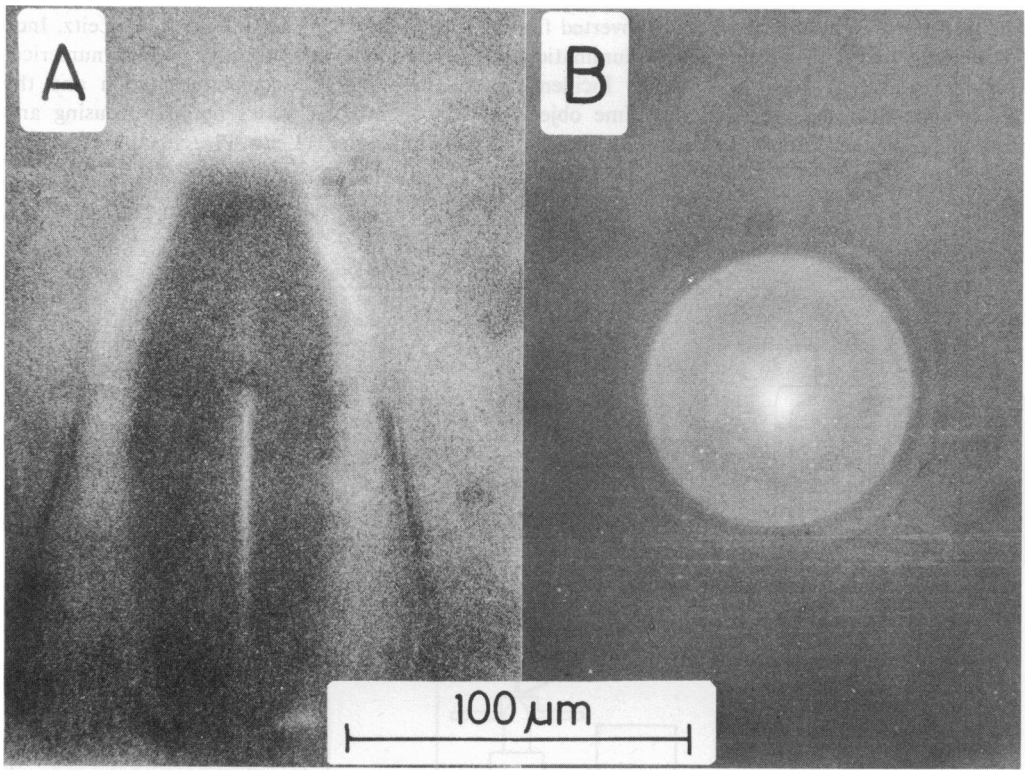

FIGURE 2 Partial view of the 360-μm Diam microscopic field showing the flow pattern in the sensor region as observed through the microscope binocular. A sample of fluorescent particles was run at oblique incidence (panel A) and vertical incidence (panel B) of the liquid jet. The parabolic contour in panel A is the outline of the liquid jet hitting the cover glass with flow direction downwards in the picture (Y-direction). The circular outline in panel B is the periphery of the 80-μm Diam liquid jet. Fluorescence from the particles in the sample flow appears as a bright line in panel A and as a bright spot in panel B. The sample flow rate was 0.013 ml/min, corresponding to a sample flow diameter of 4 μm (5 ml/min sheath flow rate). The exposure time of these photographs was several minutes. Thus, their sharpness indicates the stability of the flow pattern.

Flow System

The sheath fluid comes from a reservoir kept under 4 kg/cm^2 pressure (Fig. 3). By means of a calibrated needle valve (Whitey Co., Emeryville, Calif., SS-22RS2) the flow rate could be accurately regulated between 2 and 5 ml/min. These flow rates correspond to calculated speeds at the exit of the orifice in the range 6.5–16 m/s.

A volumetric sample delivery system[1] is operated between 0.006 ml/min and 0.060 ml/min. A step motor drives the piston of a disposable 1-ml syringe (B-D Plastipak, B-D Spear Medical Systems, Waltham, Mass.) holding the sample. A scaler counting the number of pulses going to the step motor accurately measured the sample volume delivered in a certain time interval. Before a new sample is introduced, the sample flow path is backflushed by leaving the sheath fluid running while the sample syringe is taken away, thus driving some sheath fluid from the flow chamber backwards through the sample tubing.

A small vacuum pump connected to a waste container provides the suction (½ atm) for the hypodermic needle that drains the liquid from the cover glass.

Optics

The instrument is built on a standard inverted fluorescence microscope (Leitz Diavert, E. Leitz, Inc., Rockleigh, N.J.) with incident (Epi) illumination and an oil immersion objective of high numerical aperture (Leitz, Fl 40X, N.A. 1.30). Incident illumination implies that the excitation and the fluorescence light pass through the same objective. This greatly facilitates optimal focusing and positioning of the sample stream. The incident light illuminator (Leitz Ploemopak) comprises

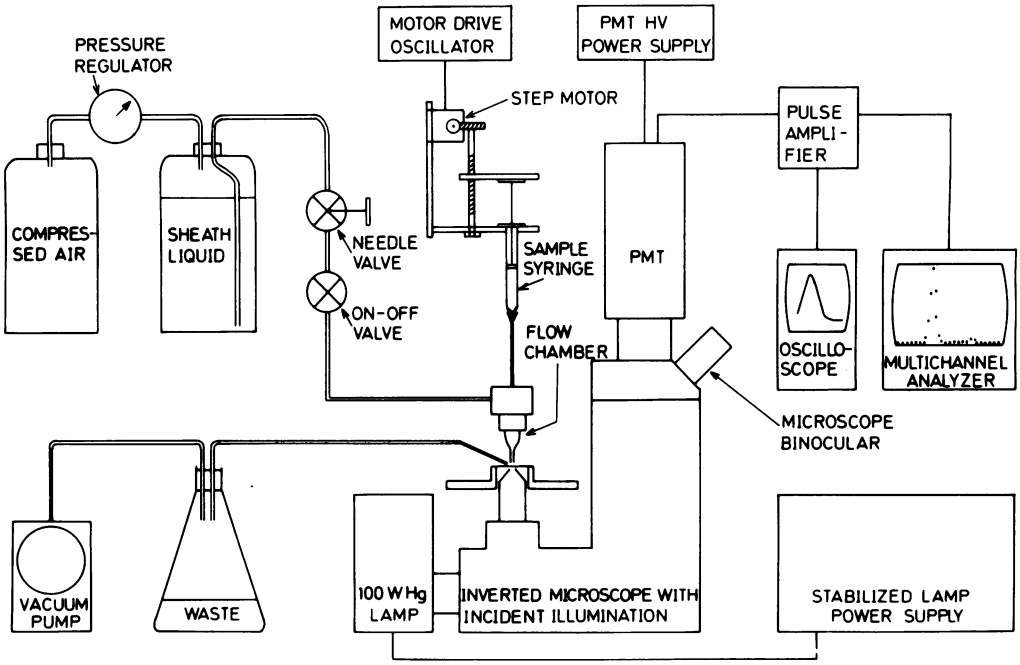

FIGURE 3 Block diagram of the flow cytometer. The micropositioning devices (X- and Y-direction) as well as the focusing device (Z-direction) of the microscope stage are not indicated.

[1]L. S. Cram and T. M. Jovin. Personal communication.

interchangeable filter sets for isolating the appropriate wavelengths of excitation and fluorescence. Filter sets are available for all commonly used fluorescent stains.

By means of an auxiliary lens (Diam 2.5 cm, f = 10 cm) placed 1.5 cm in front of the condensor of the Ploemopak illuminator, the exciting light field is concentrated to the central ⅓ Diam of the microscope field. This reduces the level of background illumination and increases the maximum excitation energy per unit area in the object plane.

The inverted microscope is equipped with a 100-W superpressure mercury lamp (Osram HBO 100, Osram GmbH., Hamburg, W. Germany) operated on DC current. Variations in illumination intensity are minimized by the electronic stabilizer circuit, shown in Fig. 4, which reduces ripple in the power supply voltage to ±1 mV and also minimizes variations in the output power.

A photomultiplier (PMT) (EMI Technology, Sunnyvale, Calif., 9659QB) mounted on the phototube of the microscope binocular converts the pulses of fluorescence into voltage pulses with amplitudes proportional to the fluorescence intensity. The effective field of view of the PMT is limited by the diameter of the excitation light field in the object plane. A frosted glass plate in front of the PMT tube spreads the light to a larger area of the PMT window.

Electronics

The pulses from the PMT are fed to a pulse amplifier (Los Alamos model 8124, [11]) operated in AC mode. The optimal time constant of the amplifier was found to be 1.2 μs for the pulses having a width at half maximum of ~3 μs. The amplifier output is connected to an oscilloscope (Tektronix Inc., Beaverton, Oreg.) where the mean pulse amplitude as well as the variation in amplitude between pulses are easily observed, thus facilitating adjustment of the instrument.

Pulses from the amplifier are also registered in a pulse height multichannel analyzer (MCA) (IN/US Service Corp., Fairfield, N.J., DIDAC 4000) such that the channel number is proportional to the pulse height. Histograms were usually registered over 1,000 channels of the MCA, with the analog-to-digital converter (ADC) operating at 100 channels/V.

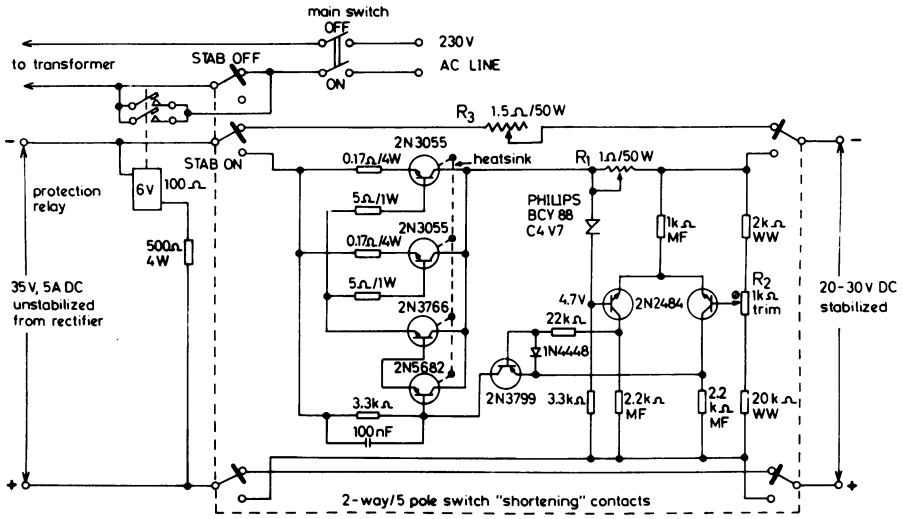

FIGURE 4 Electronic circuit for stabilizing output voltage and power from the Siemens 100-W mercury lamp power supply (Siemens Corp., Iselin, N.J.). Optimal control of output power is realized by adjusting resistor R_1 until constant output power is delivered when the circuit is connected to a variable load resistor. Normal output voltage is obtained by adjusting resistor R_2. R_3 is the control resistor originally contained in the power supply. The protection relay ensures that the lamp can be switched on only in the STAB OFF position. Shortening contacts keep the lamp burning while switching over to stabilized output. All transistors shown are made by Motorola Inc. (Southfield, Mich.).

Excellent linearity of the electronics from the amplifier to the MCA was demonstrated by giving calibrated input pulses to the amplifier under the same settings as those used for actual measurements. Regression analysis showed that the (root mean square) relative deviation from a linear relationship in channel number y as function of input pulse height x ($y = ax + b$) was only 0.3%, and the origin offset (b) was $<1/20$ of a channel interval.

INSTRUMENT PERFORMANCE

Materials and Methods

Most of the instrument testing was performed with fluorescent latex particles (Polysciences Inc., Warrington, Pa., Cat. 9847, 2.0-μm Diam) and with rat thymocytes stained with a combination of ethidium bromide (EB) and mithramycin (MI) (12) after 70% ethanol fixation. Best results were obtained when the cell concentration in the staining reaction did not exceed 10^6 cells/ml. The sample flow rate was normally ~0.01 ml/min, and the sheath fluid flow rate 5 ml/min.

Fluorescence from the latex particles as well as from cells stained with EB+MI was measured with a filter set (Ploemopak H2) which provides excitation light of wavelength 390–490 nm, and transmits fluorescence light of wavelength longer than 515 nm to the PMT. The PMT was operated at ~550–600 V.

A histogram of rat thymocytes stained with EB+MI and registered under the above-mentioned standard conditions is shown in Fig. 5. Various parameters characterizing such histograms were computed from numerical output of the data obtained on a parallel printer. The CV (relative standard deviation) was calculated from the standard deviation and mean value obtained when all channels around the peak having more than $1/10$ of the peak channel content were included in the computation. For an ideal normal distribution this corresponds to an interval of 4.3 σ around the mean value, and represents 97% of the integral of the distribution.

Results

At oblique incidence (as shown in Fig. 1), the best results were obtained when the liquid jet hit the cover glass slightly outside the field of view of the microscope. Fig. 6 shows how the CV varied with the position of the jet along the Y-axis. The optimal position of the top of the parabolic contour is ~350 μm from the center of the microscopic field. However, since the variation of CV with position of the jet is small, the performance of the instrument is essentially insensitive to a change in this parameter.

Fig. 7 shows how the CV varied with the angle of incidence. For each angle, the flow chamber was repositioned in the X- and Y-directions and the microscope was refocused (Z-direction) to obtain the optimal detection conditions. For vertical incidence, the optimal focus was slightly above the point where the liquid jet spread out on the cover glass (i.e., as shown in Fig. 2 B). Fig. 7 indicates a slight improvement of resolution as the angle of incidence was increased. At 70° angle of incidence, the best result we have obtained so far is CV = 0.9%. However, histograms with CV = 1.3% obtained at vertical incidence indicate that this configuration may also be used.

The suspension of latex particles contained a sufficient proportion of doublets to permit a reliable location of the doublet peak and calculation of its CV. The ratio of the CV of the

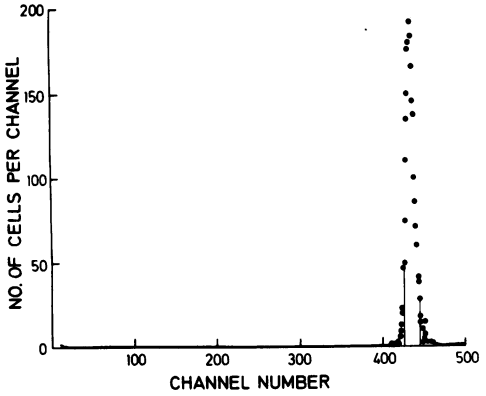

FIGURE 5

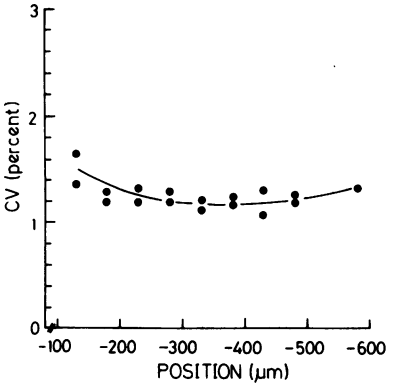

FIGURE 6

FIGURE 5 DNA histogram of rat thymocytes stained with a combination of EB+MI after 70% ethanol fixation. The histogram was registered over 1,000 channels of which the first 500 are shown. The CV was calculated from counts in the channel interval [426–445] and found to be 1.0%. The histogram was registered in 30 s, and the peak represents 2,200 cells.

FIGURE 6 CV of histograms of rat thymocytes (as in Fig. 5) obtained at 70° angle of incidence of the liquid jet as a function of its position along the *Y*-axis (Fig. 1). The abscissa indicates the position on the (negative) *Y*-axis of the top of the parabolic contour of the liquid jet (Fig. 2). The two data points at each position are independent measurements obtained after repositioning of the liquid jet.

doublet peak to that of the singlet peak was found to vary between 0.8 and 1.25, with a mean of 0.98. The ratio of the mean channel position of the doublet peak to that of the singlet peak varied within the range 1.96–2.00, with an average of 1.98. The fact that this value is slightly <2.00 is not due to the amplifier and MCA electronics, since their performance was perfectly linear (see *Electronics*). The variation in CV and position of the doublet peak relative to the singlet peak was not systematic with the angle of incidence.

For 70° angle of incidence as well as for vertical incidence the stability of the instrument was investigated by recording histograms at 5-min intervals. When using a sample of rat thymocytes, the mean channel position varied only 0.5% in a series taken over 1 h at 70° incidence, while the CV remained within 1.0–1.1%. At vertical incidence a corresponding series showed 1.5% variation in the mean channel position, with CV in the range 1.4–1.7%.

The influence of the sample flow rate and the sample analysis rate on the CV of histograms registered at 70° angle of incidence is shown in Fig. 8. Sample suspensions with three different concentrations of latex particles were used, and for each sample the analysis rate was varied by changing the sample volume flow rate. For a certain sample the CV increased with the sample volume flow rate, probably because larger variation in optical detection conditions occurred when the sample stream spread out over a wider sector in the sensor region. Furthermore, the CV increased when a higher sample analysis rate was obtained by running a more concentrated sample while keeping the sample volume flow rate fixed. The latter increase in CV was probably related to limitations in the pulse processing electronics (see below). For a certain analysis rate, a lower CV was obtained by running a more concentrated sample at a correspondingly lower sample volume flow rate. The best results seemed to be obtained if the analysis rate was $\sim 10^3$ counts/s or less and the sample volume flow rate ~0.01 ml/min (i.e., $6 \cdot 10^6$ cells/ml). Similar results were found for vertical incidence.

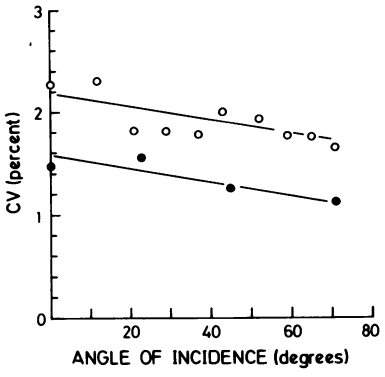

FIGURE 7

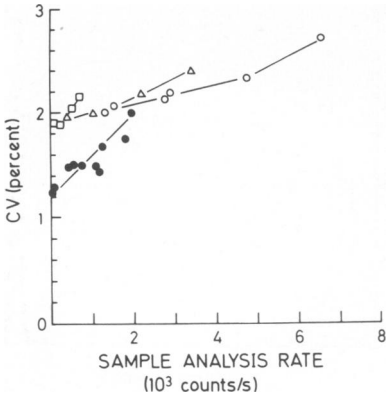

FIGURE 8

FIGURE 7 CV of histograms of rat thymocytes (●) (as in Fig. 5) and 2-μm fluorescent latex particles (○), as obtained for different angles of incidence (Fig. 1) of the liquid jet.

FIGURE 8 CV of histograms of rat thymocytes (●) (as in Fig. 5) and 2-μm fluorescent latex particles (open symbols) as obtained for different sample analysis rates at 70° angle of incidence of the liquid jet. The sample analysis rate was varied by changing particle concentration (□ = $0.5 \cdot 10^6$, △ = $2 \cdot 10^6$, ○ = 10^7 particles/ml) as well as volume flow rate of the sample (0.006/0.06 ml/min).

For analysis rates exceeding 10^3 counts/s, the mean channel position of the histogram peak decreased with increasing analysis rate. Within the series with the lower particle concentration (□, Fig. 8), there was only a 0.5% change in mean channel position. However, in the series having the higher particle concentration (○, Fig. 8) the mean channel position was reduced by 5% when the analysis rate increased from 1,500 to 6,500 counts/s. This decrease was probably an artefact caused by the electronics, since the same effect could be seen when pulses similar to those coming from the PMT were supplied to the amplifier from an electronic pulse generator. Analysis rates esceeding $2–3 \cdot 10^3$ counts/s are too high for the present electronics, since the dead time of the MCA then goes up to 10% when channel numbers around 400 are used for storage. (Pulse processing time increases with increasing channel number.) Apart from the larger CV and the lower mean channel position, the histograms were not distorted by high analysis rates.

As shown in Fig. 9, resolution is essentially independent of sheath flow rate above values of 3 ml/min. For both vertical (▲) and 70° angle of incidence (●), however, CV increased sharply when the flow rate was reduced to 2.5 ml/min. At 70° angle of incidence a 20% increase in mean channel position of the histogram peak was observed when the sheath flow rate was reduced from 5 ml/min to below 3 ml/min. This increase, which was accompanied by an increase in pulse width, occurred because, with the amplifier time constant used, there was partial integration of the pulse, leading to an increase in pulse height with pulse width.

A DNA-histogram of a proliferating cell population is shown in Fig. 10. In this case, mouse femur bone marrow cells were fixed in 70% ethanol and stained with EB+MI as for the rat thymocytes. Parameters of the DNA-histogram as well as the standard deviation of each parameter were determined by a computer program based on a mathematical model of the histogram (13). The model represents the G1 and G2+M peaks as normal distributions and the S-phase as a broadened polynomial of second degree or less. The best fit to the data was

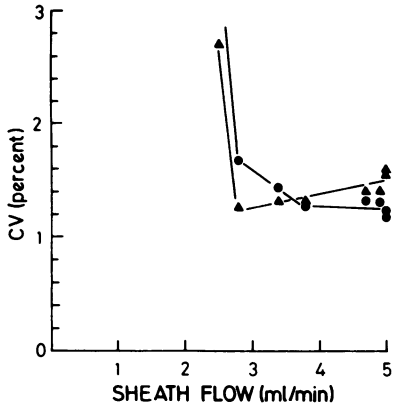

FIGURE 9

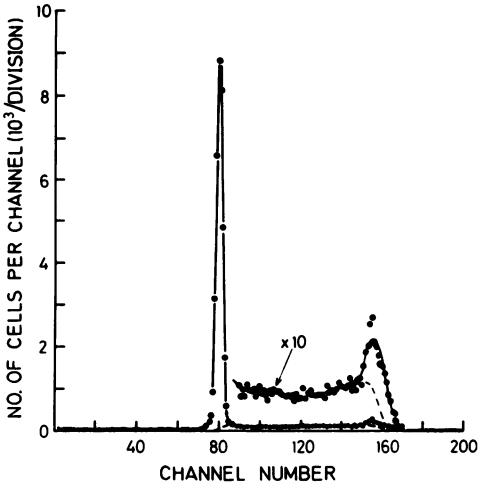

FIGURE 10

FIGURE 9 CV of histograms of rat thymocytes (as in Fig. 5) obtained at 70° (●) and vertical, i.e., 0° (▲) incidence of the liquid jet as a function of sheath fluid flow rate. A CV value of 3.9% obtained for oblique incidence at a flow rate of 2.5 ml/min is not included in the figure.

FIGURE 10 DNA histogram of mouse bone marrow cells stained with a combination of EB+MI after 70% ethanol fixation. The histogram was recorded under optimal conditions at 70° angle of incidence of the liquid jet. The fully drawn line is the histogram generated by a mathematical model that was fitted to the data by a computer program. The broken line is the model's estimate for cells in S-phase. 78% of the cells were estimated to be in G1, 18% in S, and 4% in G2+M. The CV of the G1 peak is 1.9%. The data were originally recorded over 1,000 channels, but reduced to 200 channels by combining counts from 5 channels into one. The histogram represents 44,000 cells and was recorded in 8 min.

obtained with the second degree model (Fig. 10). From the estimated model parameters the ratio between the mean positions of the G1 and G2+M peaks was found to be 1.97 and the CV of the G1 peak was 1.9%. This is a significantly larger CV than that obtained for the rat thymocytes. Such differences in CV between histograms from different cell types are commonly seen in flow cytometric DNA measurements, but their possible biological significance remains obscure. The G2+M peak of the histogram in Fig. 10 was found to be relatively broad, i.e., CV = 2.8%. Since latex particle doublets exhibited the same CV as singlets (see above), the broader G2+M peak must be due to properties of the sample rather than of the instrument.

DISCUSSION

The present instrument constitutes a robust flow cytometer that is assembled from readily available standard components.[2] The instrument is easy to operate since advantage has been taken of the mechanical and optical perfection of a modern microscope. With a resolution

[2]Some of the components of the instrument described here were installed only for the study of its detailed performance and are unnecessary in practical use. This applies to the micrometers for reproducible repositioning of the nozzle on the microscope stage, the micrometer valve in the sheath fluid flow path, and the scaler for the sample delivery system.

equal to or better than CV = 0.9% and long term stability within 1%, the instrument compares favorably with the best flow cytometers available. The above results show wide optima with regard to the various adjustable parameters, such as the position of the sample stream and the flow rates of sample suspension and sheath fluid. Hence, optimal performance is readily obtained and readjustments are rarely necessary. In our experience no readjustments are normally needed during a full day's use.

The crucial part of this flow cytometer is the new flow configuration that combines the simplicity and precision of a hydrodynamically focused sample stream in a liquid jet in air with the high numerical aperture of the oil immersion objective. Although best performance is obtained with oblique incidence of the liquid jet, i.e., 70°, good results were also found with vertical incidence, indicating that high resolution measurements are also fully feasible in the latter configuration. As noted below, each configuration may have its advantages.

A stable light source is essential for optimal performance. Thus, when the stabilizer circuit of the lamp power supply was turned off, CV increased to above 3%, and the histogram peaks became significantly distorted. Even with stabilized lamp power it appears that lamp instability, especially flicker of the discharge arc, constitutes the main limiting factor of instrumental resolution. For large angles of incidence, variations due to such factors could possibly be reduced by focusing the excitation light with a cylindrical lens to a narrow ribbon normal to the direction of sample flow. This might also give pulses of higher amplitude and smaller width, thus reducing coincidences at high analysis rates. It is possible that performance may be improved if a laser is used as a light source. However, besides the cheaper price, arc lamps such as high-pressure mercury and xenon lamps have the advantage of a wide spectrum, which makes them suitable for all stains in common use.

Irrespective of instrumental resolution, low CV values are not always observed in DNA histograms, since broadening is introduced by imperfect staining as well as by biological variability. Thus, our best DNA histograms of human peripheral lymphocytes show a CV = 1.7%, and those of proliferating mouse bone marrow cells have CV = 1.9% (Fig. 10). These results were obtained with ethanol-fixed cells stained with EB+MI (12). Staining with MI alone after ethanol fixation (14) halved the fluorescence intensity for rat thymocytes and doubled the CV.

High instrumental and experimental resolution is important in flow cytometry. For example, improvements in preparation and staining methods are greatly facilitated if variations in the CV may be observed unmasked by instrumental broadening. Flow cytometric analysis of chromosomes is another area where high resolution is essential (15).

In histograms of cellular DNA content a low CV allows a more reliable and detailed evaluation of the S-phase distribution. Thus, it has been found that the standard deviation of estimated model parameters increases exponentially with CV (13). Parameter estimates with the smallest possible standard deviations are obtained if the detail of the model is chosen in proper relation to the resolution of the data (13). For the histogram shown in Fig. 10 it was found that a second degree polynomial was the best model for representing cells in S-phase. In contrast, it has been shown that with CV in the range 5–6%, increasing the complexity of the S-phase model beyond that of a first degree function will increase the uncertainty of calculated parameters (13). For histograms with sufficiently low CV, not only the number of cells in S-phase, but also the shape of the S-phase distribution, may be reliably estimated,

thereby permitting the DNA-synthesis rate through S-phase to be derived if the age-distribution is known (16).

Several ideas for further development are associated with the present flow cytometer. It is currently being extended to two-parameter fluorescence detection by adding another PMT with necessary electronics and changing the MCA for a two-parameter analyzer. Light-scatter signals would probably not be well related to particle or cell size in the present instrument due to the large solid angle of the excitation light. However, other illumination geometries, such as dark-field incident light illumination or laser beam illumination, might facilitate light-scatter measurements. The good imaging properties of the instrument might be exploited for slit scan analysis at large angles of incidence (8, 17). Asymmetric cells become lined up with their long axis parallel to the direction of flow by the shear forces present in the hydrodynamic focusing region. If the shear forces present in the liquid jet at the point where it flattens on the cover glass further tend to orient asymmetric cells with their flat side parallel to the cover glass, then this could be utilized together with other means of cell orientation (18–22) to obtain optimal slit scan detection conditions. Vertical incidence, on the other hand, provides detection conditions free from any effects due to cell orientation (23).

The authors wish to acknowledge the skillful assistance of O. Sørensen, who constructed and built the stabilizer circuit for the lamp power supply. We are grateful for his permission to publish Fig. 4. We are indebted to L. S. Cram for valuable advice on the presentation of our work.

Received for publication 13 March 1979 and in revised form 31 May 1979.

REFERENCES

1. HORAN, P. K., and L. L. WHEELESS, JR. 1977. Quantitative single cell analysis and sorting. *Science (Wash. D.C.)*. **198**:149.
2. BARLOGIE, B., W. HITTELMAN, G. SPITZER, J. M. TRUJILLO, J. S. HART, L. SMALLWOOD, and B. DREWINKO. 1977. Correlation of DNA distribution abnormalities with cytogenetic findings in human adult leukemia and lymphoma. *Cancer Res.* **37**:4400.
3. DEAN, P. N., and D. PINKEL. 1978. High resolution dual laser flow cytometry. *J. Histochem. Cytochem.* **26**:622.
4. MEISTRICH, M. L., W. GÖHDE, R. A. WHITE, and J. SCHUMANN. 1978. Resolution of X and Y spermatids by pulse cytophotometry. *Nature (Lond.)*. **274**:821.
5. OTTO, F., and H. OLDIGES. 1978. Requirements and procedures for chromosomal DNA measurements for rapid karyotype analysis in mammalian cells. *In* Pulse Cytophotometry. D. Lutz, editor. European Press, Ghent. Part III. 393.
6. GÖHDE, W., J. SCHUMANN, Th. BÜCHNER, F. OTTO, and B. BARLOGIE. 1979. Pulse cytophotometry. Its application in tumor cell biology and clinical oncology. *In* Flow Cytometry. M. Melamed, P. F. Mullaney, and M. Mendelsohn, editors. John Wiley and Sons, New York. In press.
7. GÖHDE, W. 1973. Automation of cytofluorometry by use of the impulsmicrophotometer. *In* Fluorescence Techniques in Cell Biology. A. A. Thaer and M. Sernetz, editors. Springer Verlag, Berlin. 79.
8. GRAY, J. W., D. PETERS, J. T. MERRILL, R. MARTIN, and M. A. VAN DILLA. 1979. Slit scan flow cytometry of mammalian chromosomes. *J. Histochem. Cytochem.* **27**:441.
9. CROSLAND-TAYLOR, P. J. 1953. A device for counting small particles suspended in a fluid through a tube. *Nature (Lond.)*. **171**:37.
10. STEEN, H. B., and T. LINDMO. 1979. Flow cytometry: A high resolution instrument for everyone. *Science (Wash. D.C.)*. **204**:403.
11. STEINKAMP, J. A., M. J. FULWYLER, J. R. COULTER, R. D. HIEBERT, J. L. HORNEY, and P. F. MULLANEY. 1973. A new multiparameter separator for microscopic particles and biological cells. *Rev. Sci. Instrum.* **44**:1301.
12. BARLOGIE, B., G. SPITZER, J. S. HART, D. A. JOHNSTON, T. BÜCHNER, J. SCHUMANN, and B. DREWINKO. 1976. DNA histogram analysis of human hemopoietic cells. *Blood.* **48**:245.

13. LINDMO, T., and E. AARNÆS. 1979. Selection of optimal model for the DNA histogram by analysis of error of estimated parameters. *J. Histochem. Cytochem.* **27**:297.
14. CRISSMAN, H. A., and R. A. TOBEY. 1974. Cell-cycle analysis in 20 minutes. *Science (Wash. D.C.).* **184**:1297.
15. GRAY, J. W., A. V. CARRANO, D. H. MOORE, II, L. L. STEINMETZ, J. MINKLER, B. H. MAYALL, M. L. MENDELSOHN, and M. A. VAN DILLA. 1975. High-speed quantitative karyotyping by flow microfluorometry. *Clin. Chem.* **21**:1258.
16. GRAY, J. W., P. N. DEAN, and M. L. MENDELSOHN. 1979. Quantitative cell cycle analysis: Flow cytometry and sorting. *In* Flow Cytometry. M. Melamed, P. F. Mullaney, and M. Mendelsohn, editors. John Wiley and Sons, New York. In press.
17. WHEELESS, L. L., JR., J. A. HARDY, and N. BALASUBRAMANIAN. 1975. Slit-scan flow system for automated cytopathology. *Acta Cytol.* **19**:45.
18. KACHEL, V., E KORDWIG, and E. GLOSSNER. 1977. Uniform lateral orientation, caused by flow forces, of flat particles in flow-through systems. *J. Histochem. Cytochem.* **25**:774.
19. FULWYLER, M. J. 1977. Hydrodynamic orientation of cells. *J. Histochem. Cytochem.* **25**:781.
20. KAY, D. B., and L. L. WHEELESS, Jr. 1977. Experimental findings on gynecologic cell orientation and dynamics for three flow nozzle geometries. *J. Histochem. Cytochem.* **25**:870.
21. STOVEL, R. T., R. G. SWEET, and L. A. HERZENBERG. 1978. A means for orienting flat cells in flow systems. *Biophys. J.* **23**:1.
22. DEAN, P. N., D. PINKEL, and M. L. MENDELSOHN. 1978. Hydrodynamic orientation of sperm heads for flow cytometry. *Biophys. J.* **23**:7.
23. VAN DILLA, M. A., B. L. GLEDHILL, S. LAKE, P. N. DEAN, J. W. GRAY, V. KACHEL, B. BARLOGIE, and W. GÖHDE. 1977. Measurement of mammalian sperm deoxyribonucleic acid by flow cytometry. Problems and approaches. *J. Histochem. Cytochem.* **25**:763.